

Asymmetric centrosome inheritance maintains neural progenitors in the neocortex

Xiaoqun Wang¹, Jin-Wu Tsai², Janice H. Imai^{1,3}, Wei-Nan Lian², Richard B. Vallee² & Song-Hai Shi^{1,3}

Asymmetric divisions of radial glia progenitors produce self-renewing radial glia and differentiating cells simultaneously in the ventricular zone (VZ) of the developing neocortex. Whereas differentiating cells leave the VZ to constitute the future neocortex, renewing radial glia progenitors stay in the VZ for subsequent divisions. The differential behaviour of progenitors and their differentiating progeny is essential for neocortical development; however, the mechanisms that ensure these behavioural differences are unclear. Here we show that asymmetric centrosome inheritance regulates the differential behaviour of renewing progenitors and their differentiating progeny in the embryonic mouse neocortex. Centrosome duplication in dividing radial glia progenitors generates a pair of centrosomes with differently aged mother centrioles. During peak phases of neurogenesis, the centrosome retaining the old mother centriole stays in the VZ and is preferentially inherited by radial glia progenitors, whereas the centrosome containing the new mother centriole mostly leaves the VZ and is largely associated with differentiating cells. Removal of ninein, a mature centriole-specific protein, disrupts the asymmetric segregation and inheritance of the centrosome and causes premature depletion of progenitors from the VZ. These results indicate that preferential inheritance of the centrosome with the mature older mother centriole is required for maintaining radial glia progenitors in the developing mammalian neocortex.

Radial glia cells constitute a major population of neural progenitor cells that occupy the proliferative VZ in the developing mammalian neocortex^{1–3}. In addition to their well-characterized function as a scaffold in supporting neuronal migration⁴, radial glia cells display interkinetic nuclear oscillation and proliferate extensively at the luminal surface of the VZ (that is, the VZ surface). During the peak phase of neurogenesis (around embryonic day 13–18 (E13–E18) in mice) they predominantly undergo asymmetric division to self-renew while simultaneously giving rise either directly to a neuron, or to an intermediate progenitor cell which subsequently divides symmetrically to produce neurons^{5–8}. Whereas differentiating progeny progressively migrate away from the VZ to form the cortical plate (CP)—the future neocortex—renewing radial glia progenitors remain in the VZ for subsequent divisions. The distinct migratory behaviour of radial glia progenitors and their differentiating progeny is fundamental to the proper development of the mammalian neocortex; however, little is known about the basis of these behavioural differences.

Centrosomes, the main microtubule-organizing centres in animal cells⁹, have an important role in many cell processes, particularly during cell division¹⁰ and cell migration^{11–13}. All normal animal cells initially inherit one centrosome, consisting of a pair of centrioles surrounded by an amorphous pericentriolar material. The two centrioles differ in their structure and function^{9,14,15}. The older ‘mother’ centriole, which is formed at least one-and-a-half generations earlier, possesses appendages/satellites that bear specific proteins, such as cenexin (also known as Odf2)^{16,17} and ninein^{18–20}, and anchor microtubules and support ciliogenesis^{9,21}. In contrast, the younger ‘daughter’ centriole, which is formed during the preceding S phase, lacks these structures. Full acquisition of appendages/satellites by the

daughter centriole is not achieved until at least one-and-a-half cell cycles later^{22,23}. During each cell cycle, the centrosome replicates once in a semi-conservative manner²⁴, resulting in the formation of two centrosomes: one of which retains the original old mother centriole (that is, the mother centrosome) while the other receives the new mother centriole (that is, the daughter centrosome)^{14,15}. This intrinsic asymmetry in the centrosome has recently been demonstrated to be important for proper spindle orientation during the division of male germline stem cells^{25,26} and neuroblasts^{27,28} in *Drosophila*, although female germline stem cells appear to divide normally in the absence of centrioles/centrosomes²⁹. These studies indicate a critical role for the differential behaviour of centrosomes with differently aged mother centrioles in asymmetric division of the progenitor/stem cells^{30–33}, although it remains unclear whether proper behaviour and development of the progenitor/stem cells and their differentiating daughter cells depend on centrosome asymmetry. Asymmetric division of radial glia progenitors accounts for nearly all neurogenesis in the developing mammalian neocortex^{5–8}. Three out of four autosomal recessive primary microcephaly (MCPH) genes identified so far encode centrosomal components³⁴, suggesting that proper neocortical neurogenesis and development entail a tight regulation of the centrosome³⁵, which is so far poorly understood. To address these issues, we investigated centrosome regulation during the peak phase of mammalian neocortical neurogenesis (Supplementary Fig. 1).

Centriole and centrosome asymmetry

To examine centrosome behaviour, we introduced a plasmid encoding centrin 1, a central component of the centriole, fused with enhanced green fluorescent protein (EGFP–CETN1) into the developing

¹Developmental Biology Program, Memorial Sloan Kettering Cancer Centre, 1275 York Avenue, New York, New York 10065, USA. ²Departments of Pathology and Cell Biology, Columbia University, 630 W. 168th Street, New York, New York 10032, USA. ³BCMB Allied Program, Weill Cornell Medical College, 1300 York Avenue, New York, New York 10065, USA.

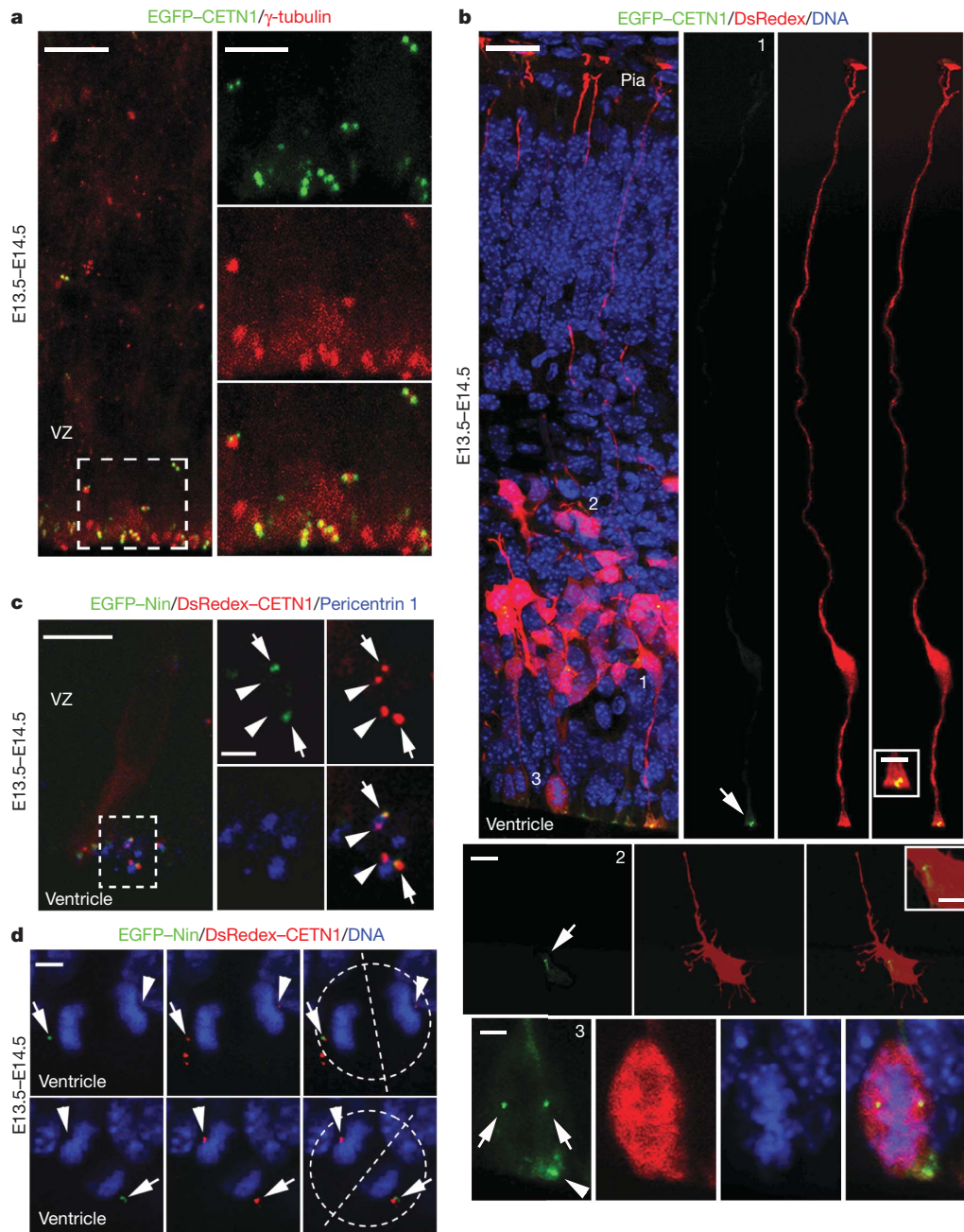


Figure 1 | Centriole and centrosome asymmetry in the developing neocortex. **a**, Images of E14.5 cortices electroporated with EGFP-CETN1 (green) at E13.5 (E13.5–E14.5) and immunostained for γ -tubulin (red). **b**, Images of cortices electroporated with EGFP-CETN1 (green) and DsRedex (DsRedex, red) and counterstained with DAPI (blue). Arrows and the arrowhead indicate the centrosomes. Pia represents the pial surface of the neocortex. **c**, Images of cortices electroporated with EGFP-Nin (green,

arrows) and DsRedex-CETN1 (red, arrows and arrowheads) and immunostained for pericentrin 1 (blue). **d**, Images of dividing radial glia cells in late mitosis (broken circles) with condensed chromosomes (DAPI, blue) expressing EGFP-Nin (green, arrows) and DsRedex-CETN1 (red, arrows and arrowheads). Broken lines indicate the cleavage plane. Scale bars: **a**, 10 μ m and 5 μ m; **b**, 25 μ m, 2.5 μ m, 10 μ m, 5 μ m and 5 μ m (from top to bottom); **c**, 20 μ m and 2 μ m; **d**, 5 μ m.

neocortex of E13.5 mouse embryos by *in utero* electroporation (Supplementary Fig. 2a). As expected, EGFP-CETN1 formed pairs of dots that co-localized with γ -tubulin, a centrosomal marker (Fig. 1a), suggesting that transient expression of EGFP-CETN1 reliably labels the two centrioles of individual centrosomes in the developing neocortex *in vivo*. Moreover, we observed that at the onset of peak neurogenesis (E13–E14), EGFP-CETN1-labelled centrosomes were predominantly located at the VZ surface with a small subset located in the subventricular zone (SVZ) and the intermediate zone (IZ) (Fig. 1a and Supplementary Fig. 2b).

To identify the cell types harbouring EGFP-CETN1-labelled centrosomes, we co-electroporated a plasmid encoding DsRedex

(DsRedex), a red fluorescent protein that diffuses throughout cells and thereby reveals their morphology (Fig. 1b). We found that in bipolar radial glia progenitors in the VZ the centrosome was located in their ventricular endfeet at the VZ surface (Fig. 1b, cell 1) as previously suggested^{36,37}, whereas in multipolar cells in the IZ and the SVZ the centrosome was harboured in their cell bodies (Fig. 1b, cell 2). Moreover, we observed dividing radial glia progenitors that possess a pair of centrosomes together with condensed chromosomes at the VZ surface (Fig. 1b, cell 3). Consistent with this differential centrosome localization between radial glia progenitors and their differentiating daughter cells, we observed a progressive increase in the appearance of EGFP-CETN1-labelled centrosomes in the IZ and

the CP as development proceeded, in addition to some that remained at the VZ surface (Supplementary Fig. 2b, c). This gradual increase in centrosome localization in the IZ and the CP coincided with the production and migration of differentiating cells such as neurons to these regions during this period.

The distinct positioning of the centrosome in radial glia progenitors versus their differentiating progeny prompted us to ask whether the centrosomes in these two cell populations/types are different. To explore this, we electroporated a plasmid encoding ninein, a mature centriole-specific protein that localizes to appendages/satellites^{18,19}, fused with EGFP (EGFP–Nin) together with a plasmid encoding CETN1 fused to DsRedex (DsRedex–CETN1) into the developing mouse neocortex at E13.5. As expected, both EGFP–Nin and DsRedex–CETN1 formed dot-like structures and co-localized to the centrosomes, especially those at the VZ surface, as identified by an antibody to the integral centrosomal protein pericentrin 1 (Fig. 1c). Notably, EGFP–Nin was preferentially concentrated at one of the two centrioles marked by DsRedex–CETN1 in individual centrosomes (Fig. 1c), suggesting that the two centrioles in interphase radial glia progenitors are not identical. Given that Nin specifically associates with mature centrioles^{18–20}, these results indicate that the centriole with abundant EGFP–Nin is the more mature mother centriole, whereas the one with little EGFP–Nin is the less mature daughter centriole. A similar inequity in the recruitment of EGFP–Nin by the duplicated centrosomes was also observed in dividing radial glia progenitors at the VZ surface (Fig. 1d), indicating that the duplicated centrosomes are not identical during late mitosis. The centrosome with abundant EGFP–Nin is probably the centrosome that retains the mature old mother centriole and the centrosome with little EGFP–Nin is probably the centrosome that bears the relatively immature new mother centriole.

Having found that the centrosomes in dividing radial glia progenitors exhibit asymmetry in their maturity, we next asked whether this centrosome asymmetry is related to the distinct behaviour of radial glia progenitors and their differentiating progeny in the developing neocortex during neurogenesis. To address this, we compared the relative distribution of centrosomes labelled by DsRedex–CETN1 versus those labelled by EGFP–Nin in the developing neocortex as development proceeded (Supplementary Fig. 3). Interestingly, whereas DsRedex–CETN1-labelled centrosomes progressively occupied the IZ and the CP, where differentiating cells are situated, EGFP–Nin-labelled centrosomes were mostly found in the VZ, where radial glia progenitors are located. Given that DsRedex–CETN1 labels all centrosomes whereas EGFP–Nin selectively labels mature centrosomes, these results point to an intriguing possibility that the duplicated centrosomes in dividing radial glia cells are differentially inherited depending on their age and maturity during neocortical neurogenesis. It is known that during each cell division one centrosome retains the old mature mother centriole and the other bears the new less mature mother centriole^{14,15,22,38}. Thus, these results suggest that centrosomes with differently aged mother centrioles are differentially inherited by the two daughter cells of asymmetrically dividing radial glia progenitors.

In vivo pulse-chase labelling of centrosomes

To test this, we first developed an assay to distinguish explicitly between the centrosome containing the old mother centriole and the centrosome containing the new mother centriole in the developing neocortex *in vivo* (Fig. 2a, b). The assay takes advantage of the photoconvertible fluorescent protein Kaede³⁹, which changes from green to red fluorescence on exposure to violet light. Centrioles in the developing neocortex were labelled by transient expression of CETN1 fused with Kaede (Kaede–CETN1). Photoconversion was then performed to switch labelled centrioles from green to red fluorescence. This green-to-red fluorescence conversion of Kaede proteins is irreversible and the red protein is very stable³⁹, thus allowing long-term tracking of the existing photoconverted proteins and the structures with which they are associated. Moreover, all newly synthesized Kaede proteins

are green fluorescent. It is known that centriole duplication requires new protein synthesis of centrin⁴⁰. As a result, newly duplicated centrioles that contain newly synthesized Kaede–CETN1 are green fluorescent, whereas previously existing centrioles are red fluorescent. Hence, in the first cell cycle after photoconversion, both centrosomes contain a red fluorescent mother centriole and a green fluorescent daughter centriole. However, in the second and subsequent cell cycles, centrosomes with the new mother centriole contain only green fluorescent centrioles, whereas centrosomes retaining the original old mother centriole harbour both red and green fluorescent centrioles, thus distinguishing between centrosomes with differently aged mother centrioles (Fig. 2a).

To carry out this assay in the developing neocortex *in vivo*, we developed an *in utero* photoconversion procedure and combined it with *in utero* electroporation (Fig. 2b). Kaede–CETN1, which localized specifically to the centrosomes (Supplementary Fig. 4), was introduced into the developing mouse neocortex at E13.5. One day later, that is, E14.5, the forebrain of electroporated embryos was treated with a short exposure of violet light while still in the uterus, which effectively converted nearly all Kaede–CETN1 proteins and their labelled centrosomes from green to red fluorescence (E13.5–E14.5(PC), Supplementary Fig. 5a, b). The uterus was replaced and the embryos continued to develop *in vivo*. The localization and inheritance of centrosomes were analysed at different developmental stages thereafter.

We found that one day after photoconversion (E13.5–E14.5(PC)–E15.5), around 95% of centrosomes contained both red and green fluorescent centrioles (indicated by yellow colour in the merged image) (Supplementary Fig. 5c, d), consistent with the notion that the labelled cells have undergone one round of division and have duplicated their centrioles during the 24-h period after photoconversion. This was shown directly by imaging centrosomes at high magnification (Supplementary Fig. 6), revealing that each centriole was mostly only red or green fluorescent. This also demonstrates that there is little diffusion of centrin proteins between duplicated centrioles, or between the centrioles and a cytoplasmic pool which was confirmed by fluorescence recovery after photobleaching (FRAP) experiments (Supplementary Fig. 7). Moreover, we found that more than 30% of centrosomes possessed only green fluorescent centrioles 2 days after photoconversion (E13.5–E14.5(PC)–E16.5) (Fig. 2c, d). The appearance of the solely green fluorescent centrosomes 48 h after photoconversion indicates that the initially labelled radial glia progenitors have undergone two rounds of division during this period; this is consistent with the previous observation that the duration of the neocortical progenitor cell cycle is about 12 to 20 h around this developmental stage⁴¹. The ongoing division of labelled radial glia cells at a normal rate suggests that expression of Kaede–CETN1 and the photoconversion procedure had no effect on their cell cycle. In addition, no obvious DNA damage or cell death was induced by the photoconversion treatment (Supplementary Fig. 8). Besides the green and yellow fluorescent centrosomes, we observed about 4% of solely red fluorescent centrosomes (Fig. 2d), indicating that a few labelled cells do not undergo cell division during this period.

Asymmetric segregation and inheritance of centrosomes

Having successfully distinguished the centrosomes with differently aged mother centrioles in the developing neocortex *in vivo*, we next examined their distribution to determine whether they are asymmetrically segregated. Remarkably, we found that more than 76% of centrosomes with the new mother centriole (that is, only green fluorescent) were located in the IZ and the CP, whereas around 78% of centrosomes with the old mother centriole (that is, both green and red fluorescent) were located in the VZ in addition to the SVZ (Fig. 2c, e, f). These results demonstrate that the centrosomes with differently aged mother centrioles are asymmetrically segregated in the developing neocortex during the peak phase of neurogenesis. It is worth noting that a small fraction of both green and red (that is, yellow) fluorescent centrosomes was found in the IZ and the CP

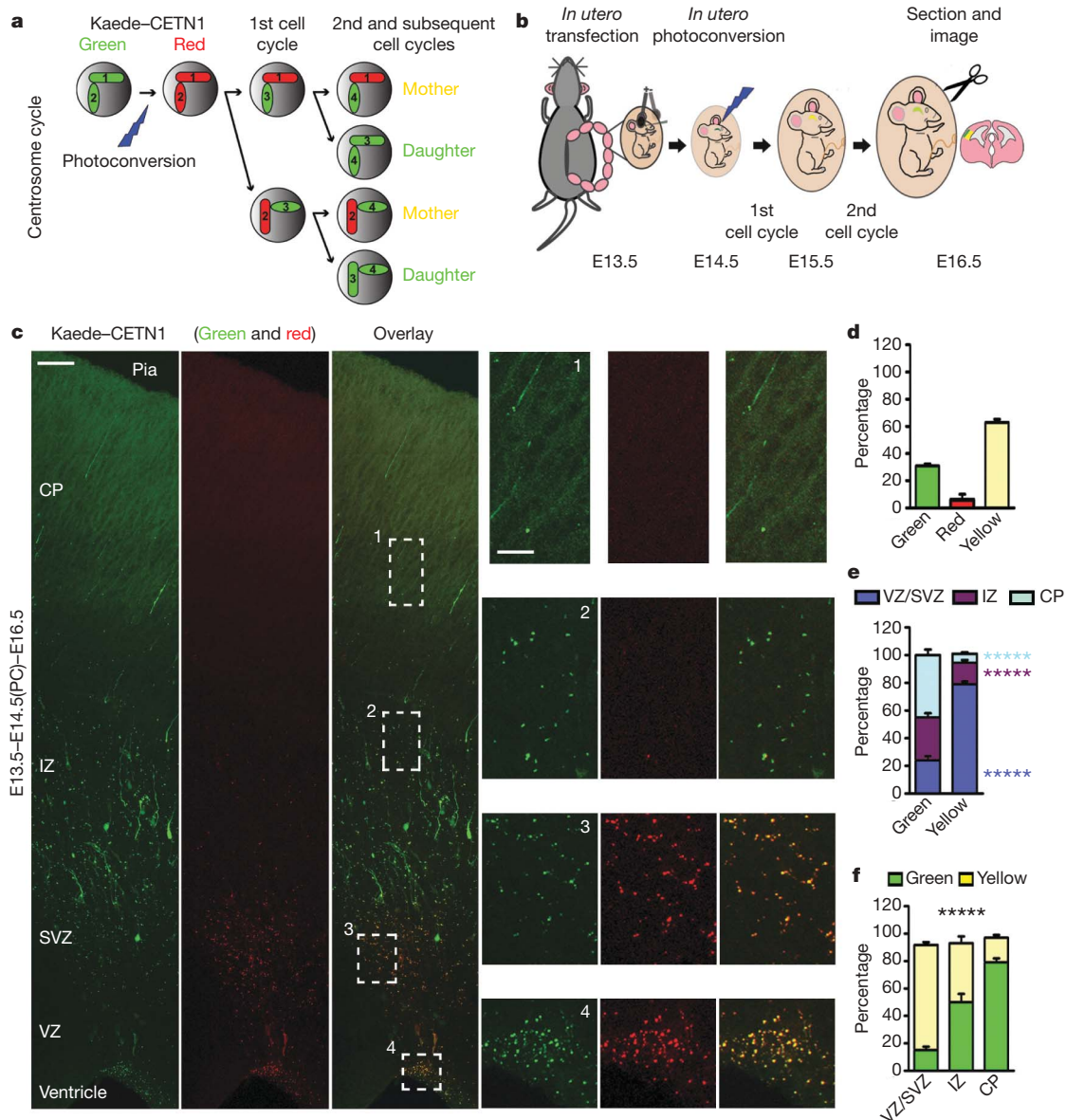


Figure 2 | Asymmetric segregation of centrosomes with differently aged mother centrioles. **a, b,** Strategy and experimental procedure for using Kaede-CENTN1 to distinguish between centrosomes with differently aged mother centrioles. **c,** Images of E16.5 cortices electroporated with Kaede-CENTN1 at E13.5 and photoconverted (PC) at E14.5 (E13.5–E14.5(PC)–E16.5). Scale bars: 50 μ m and 15 μ m. **d–f,** Quantifications of the percentage of labelled centrosomes that are green, red or yellow

(Fig. 2e, f) and that these centrosomes probably originated from the first cell cycle after photoconversion (Supplementary Fig. 5c, d).

The asymmetric segregation of centrosomes suggests differential regulation of the duplicated centrosomes in dividing radial glia progenitors. To gather further evidence for this, we carried out time-lapse imaging experiments to monitor the behaviour of centrosomes with differently aged mother centrioles in dividing radial glia progenitors at the VZ surface *in situ* (Fig. 3a). Kaede-CENTN1 was introduced into radial glia cells together with mPlum, a far-red fluorescent protein, to label cell morphology. Around 24 h later, cortical slices were prepared. Photoconversion of the existing Kaede-CENTN1 proteins was then performed in individual slices, which were then cultured for another 24 h before being subjected to time-lapse imaging. Labelled dividing radial glia cells with enlarged and rounded cell bodies possessing a pair of centrosomes at the VZ surface (Fig. 3b) were monitored at 10-min intervals over a period of 5 to 8 h (Fig. 3c, d, Supplementary Video 1 and Supplementary Fig. 9). In six out of seven dividing radial glia cells that proceeded through

mitosis at the VZ surface and reached the two-cell stage, the centrosome retaining the old mother centriole in both red and green fluorescence stayed at the VZ surface, whereas the centrosome containing the new mother centriole in solely green fluorescence migrated away from the VZ surface (Fig. 3c, d, Supplementary Video 1 and Supplementary Fig. 9). These results demonstrate that the centrosomes with differently aged mother centrioles in dividing radial glia progenitors exhibit distinct behaviour during the peak phase of neurogenesis.

The distinct behaviour of the centrosomes suggests that they are differentially inherited by the two daughter cells embarking on different routes of fate specification and development. On the basis of their behaviour, we postulated that the centrosome with the new mother centriole is largely inherited by differentiating cells, such as neurons, whereas the centrosome with the old mother centriole that remains located at the VZ is mostly inherited by radial glia progenitors. Indeed, we found that 2 days after photoconversion (E13.5–E14.5(PC)–E16.5) the centrosomes with the new mother centriole, marked by green

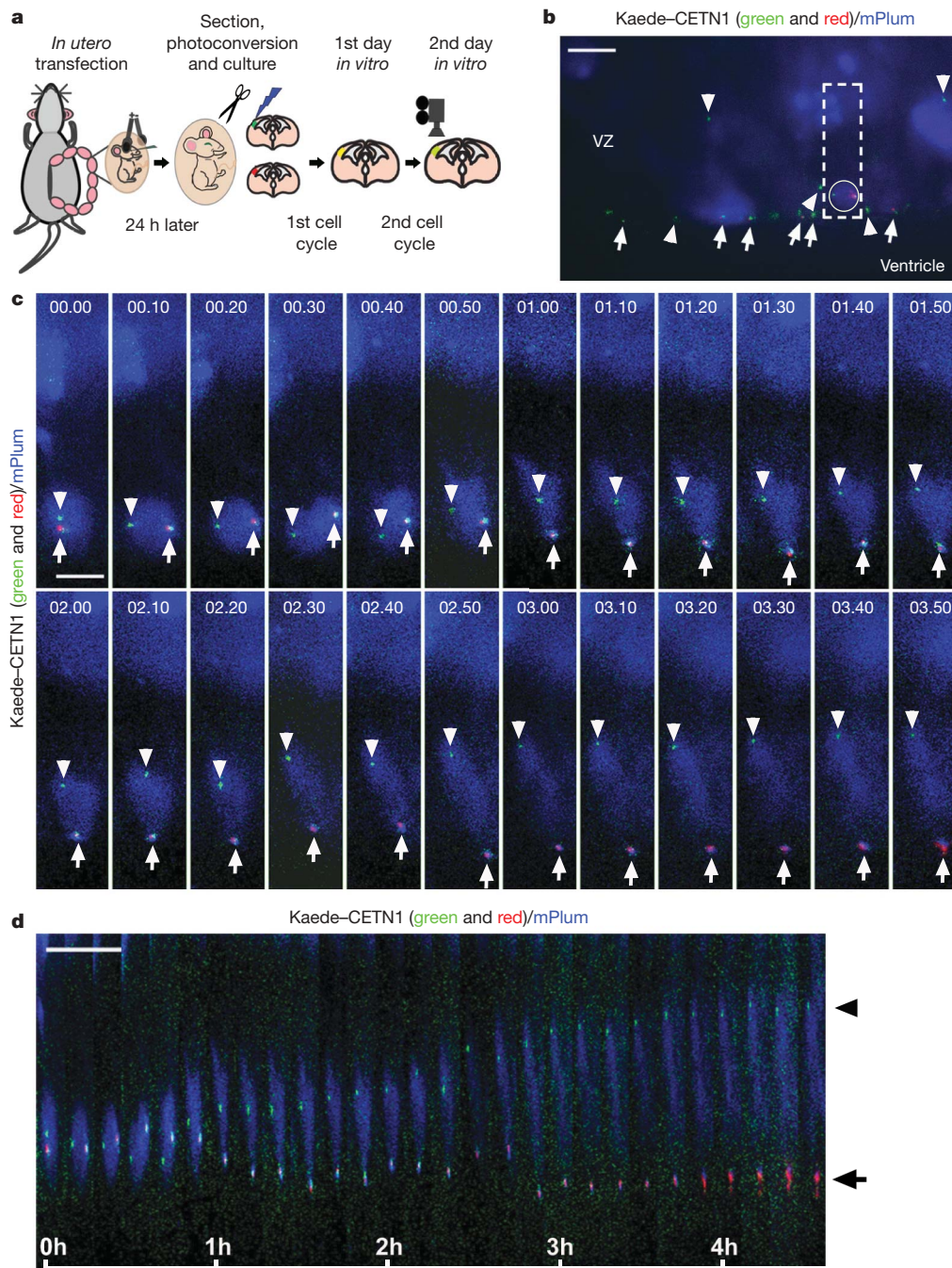


Figure 3 | Distinct behaviour of centrosomes with differently aged mother centrosomes. **a**, Experimental procedure for time-lapse imaging analysis of centrosome behaviour. **b**, Image of a cortical slice in culture expressing Kaede-CETN1 (green and red) and mPlum (blue) before time-lapse imaging. Arrows indicate the centrosomes with the old mother centriole (both green and red fluorescent) and arrowheads indicate the centrosomes with the new mother centriole (green fluorescent only). The outlined region

fluorescence alone, were mostly associated with cells expressing TUJ1, a differentiating neuronal marker, in the CP and the IZ (Fig. 4a). In contrast, the centrosomes that retained the old mother centriole in yellow (that is, both green and red) fluorescence at the VZ were largely associated with cells expressing Pax6, a radial glia progenitor marker (Fig. 4b). These results show that the centrosomes with differently aged mother centrioles in dividing radial glia cells are asymmetrically inherited by the two daughter cells: whereas the renewing radial glia progenitor inherits the centrosome with the old mother centriole, the differentiating daughter cell inherits the centrosome with the new mother centriole.

contains a dividing radial glia cell possessing a pair of centrosomes with differently aged mother centrioles (circled). **c**, **d**, Time-lapse (**c**) and kymograph (**d**) images of the outlined region in **b**. The time is indicated at the top (**c**) or the bottom (**d**) of images (in hours and minutes). Arrows indicate centrosomes possessing the old mother centriole and arrowheads indicate centrosomes possessing the new mother centriole. Scale bars: **b**, 15 μm ; **c**, **d**, 10 μm .

Asymmetric centrosome inheritance maintains progenitors

Our data thus far show that centrosomes with differently aged mother centrioles are differentially inherited by the two daughter cells of asymmetrically dividing radial glia progenitors in the developing neocortex. We next tested whether the selective inheritance of the centrosome with the old mature mother centriole by radial glia progenitors is necessary for their maintenance at the VZ. Should this be the case, given that Nin is an essential component of the appendage/satellite structures specific to the mature centriole, we predicted that removal of Nin, which prevents centriole maturation^{19,42}, would disrupt asymmetric segregation of centrosomes with differently aged

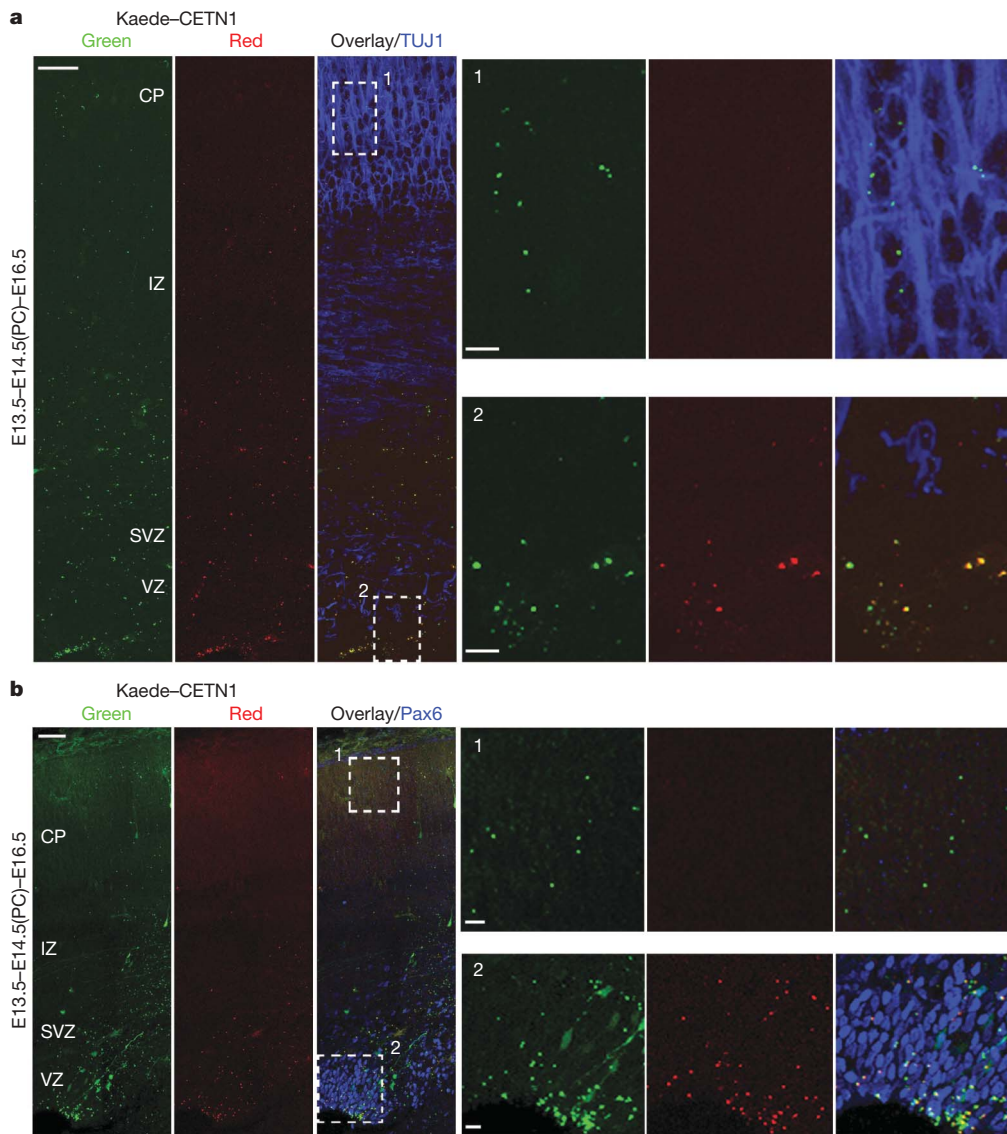


Figure 4 | Asymmetric inheritance of centrosomes with differently aged mother centrioles. Images of cortices electroporated with Kaede-CETN1, photoconverted and immunostained for TUJ1 (**a**) or for Pax6 (**b**) (blue).

High magnification images of the outlined regions are shown to the right. Scale bars: 50 μ m, 10 μ m and 10 μ m.

mother centrioles and impair the maintenance of radial glia progenitors in the developing neocortex.

To test this, we developed short hairpin RNA (shRNA) sequences against *Nin* that effectively suppressed its expression (*Nin* shRNAs, Supplementary Fig. 10a). Consistent with our prediction, expression of *Nin* shRNA, but not control shRNA, disrupted asymmetric segregation of centrosomes with differently aged mother centrioles labelled with Kaede-CETN1 in the developing neocortex (Supplementary Fig. 11), suggesting that *Nin* is necessary for centriole maturation, thereby generating asymmetry between duplicated centrosomes. The presence of solely green fluorescent centrosomes in *Nin* shRNA-expressing cortices indicates that centrosome duplication and segregation and cell division are not severely affected by removal of *Nin*, as suggested previously^{19,42}. More importantly, we found that removal of *Nin* caused a premature depletion of cells from the VZ, where radial glia progenitors reside (Fig. 5a, b). This effect of *Nin* shRNAs correlated with their efficacy in suppressing *Nin* protein expression (Supplementary Fig. 10a, b) and was rescued by a shRNA-insensitive *Nin* plasmid (Supplementary Fig. 10c), suggesting that the effect of the *Nin* shRNA is due to a specific depletion of the endogenous *Nin* protein. A similar reduction in cells in the VZ was

observed when *Nin* expression was suppressed using small interfering RNA (siRNA) (Supplementary Fig. 10d, e).

To characterize further the extent to which removal of *Nin* leads to a depletion of radial glia progenitors, we next examined the fate specification of cells expressing either control or *Nin* shRNA (Fig. 5c–f). When compared with the control, expression of *Nin* shRNA led to a marked reduction in the percentage of cells positive for Pax6 and glutamate transporter (GLAST) (Fig. 5c, d and Supplementary Fig. 12), two radial glia progenitor markers, and a significant increase in the percentage of cells positive for TUJ1 (Fig. 5e, f), a differentiating neuronal marker. These results suggest that removal of *Nin* leads to a depletion of radial glia progenitors and a concomitant increase in differentiating neurons. Consistent with this, we observed a significant reduction in phosphohistone 3 (P-H3)-labelled mitotic cells at the VZ surface (Supplementary Fig. 13) and a marked increase in cell cycle exit (Supplementary Fig. 14). No obvious change in the cleavage plane orientation of late stage mitotic cells at the VZ surface was observed (Supplementary Fig. 15).

Previous studies showed that the carboxy-terminus of *Nin* is responsible for its localization to the centriole and expression of this region displaces endogenous protein at the centriole⁴³. Interestingly, we found that, similar to removal of *Nin*, expression of the carboxy-terminus of

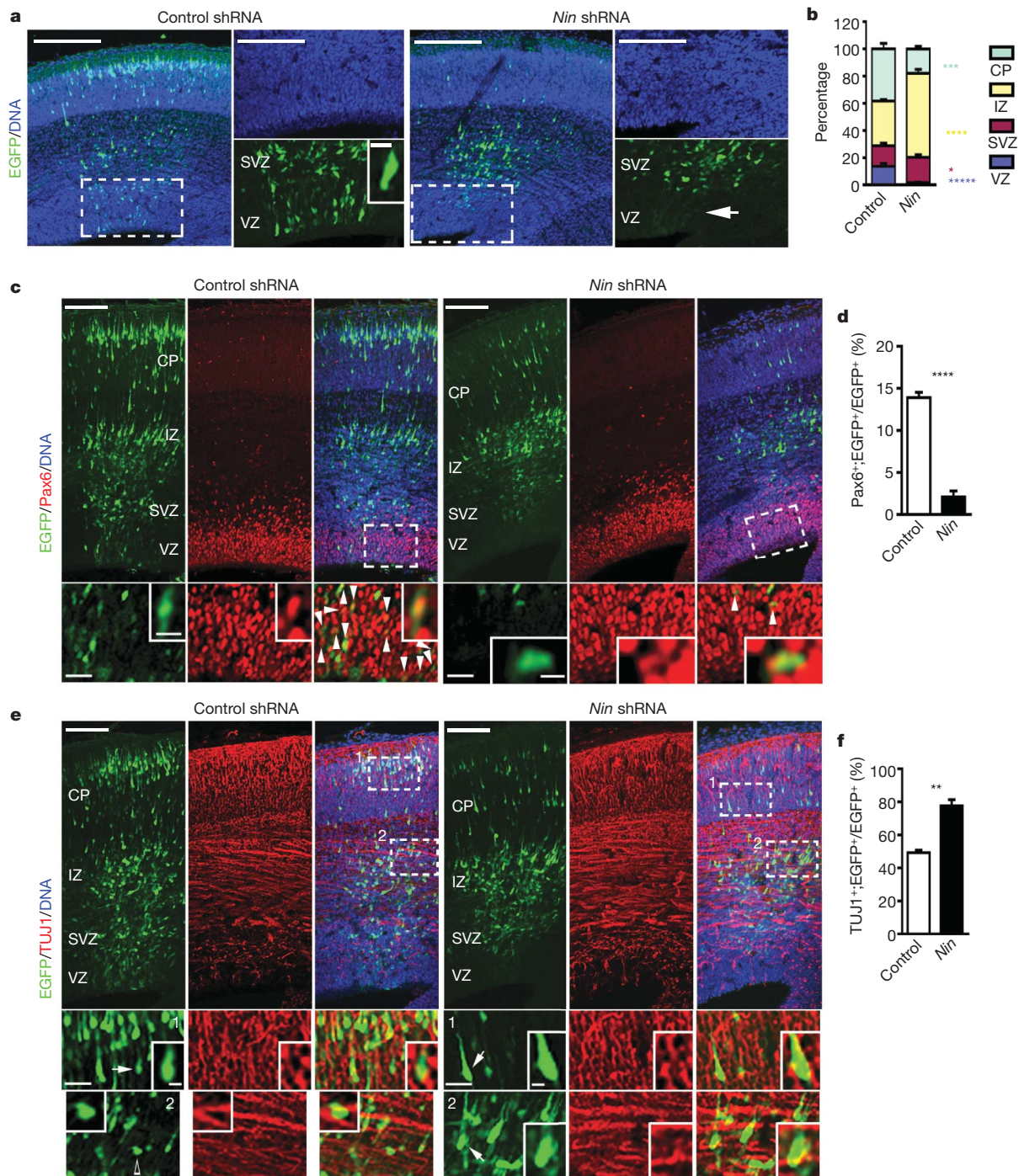


Figure 5 | Preferential inheritance of the centrosome with the mature mother centriole maintains radial glia progenitors. **a**, Images of E16.5 cortices electroporated with either EGFP/control (left, green) or EGFP/*Nin* shRNA (right, green) at E13.5 and counterstained with DAPI (blue). **b**, Quantification of the percentage of EGFP-expressing cells in different regions of the developing neocortex (control shRNA, total 1,873 cells from five individual animals; *Nin* shRNA, total 958 cells from five individual animals). **c**, **e**, Images of E16.5 cortices electroporated with EGFP/control (left, green) or EGFP/*Nin* shRNA (right, green) at E13.5 and immunostained for Pax6 (**c**) or TUJ1 (**e**) (red). Arrowheads indicate EGFP-expressing cells

positive for Pax6 (**c**). Arrows indicate EGFP-expressing cells that are positive for TUJ1 and the open arrowhead indicates an EGFP-expressing cell that is not positive for TUJ1 (**e**). **d**, **f**, Quantification of the percentage of EGFP-expressing cells positive for Pax6 (**d**; control shRNA, total 1,752 cells from five individual animals; *Nin* shRNA, total 1,230 cells from five animals) or for TUJ1 (**f**; control shRNA, total 1,383 cells from five individual animals; *Nin* shRNA, total 1,247 cells from five individual animals). Data are shown as mean \pm s.e.m.; *, $P < 0.05$; **, $P < 0.005$; ***, $P < 0.001$; ****, $P < 0.0005$; *****, $P < 5 \times 10^{-5}$. Scale bars: **a**, 100 μ m, 50 μ m and 10 μ m; **c**, 100 μ m, 5 μ m and 25 μ m; **e**, 100 μ m, 25 μ m and 5 μ m.

Nin (*Nin*-Cter) led to a premature depletion of radial glia progenitor cells from the VZ (Supplementary Fig. 16), suggesting that centriolar *Nin* is critical for maintaining radial glia progenitor cells in the VZ. Taken together, these results indicate that preferential inheritance of a centrosome containing the mature mother centriole is required for the

maintenance of radial glia progenitors in the proliferative VZ of the developing neocortex.

The results presented here suggest that the centrosomes with differently aged centrioles in asymmetrically dividing radial glia progenitors exhibit different behaviour and are differentially inherited by the

two daughter cells during the peak phase of mammalian neocortical neurogenesis (Supplementary Fig. 1). Whereas the centrosome with the less mature new mother centriole migrates away from the VZ surface and is largely inherited by differentiating cells, the centrosome with the more mature old mother centriole stays at the VZ surface and is predominantly inherited by renewing radial glia progenitors. Recently, asymmetric behaviour of centrosomes has been observed during asymmetric division of *Drosophila* male germline stem cells and neuroblasts^{25–28}. Our findings suggest that this type of asymmetric centrosome regulation may be a general feature of asymmetric cell division across species^{30–33}. Furthermore, our findings provide new insight into centrosome regulation in the developing mammalian neocortex, which has been linked to the pathogenesis of human microcephaly^{34,44}.

Centrosomes with differently aged mother centrioles differ in their protein composition and thereby in their biophysical properties, such as microtubule anchorage activity^{9,15} and the capability to mediate ciliogenesis^{21,23,45}. In this study, we found that Nin, an appendage/satellite-specific protein required for centriole maturation, localized differently to the duplicated centrosomes in radial glia progenitors in late mitosis. Notably, another appendage/satellite-specific protein cenexin was recently found to be asymmetrically localized to centrosomes in sister cells after mitosis; moreover, the cell receiving the more mature old mother centriole usually grew a primary cilium first²¹. The asymmetric inheritance of centrosomes with distinct biophysical properties may thereby differentially regulate the behaviour and development of the daughter cells that receive them. For example, given that primary cilia have essential roles in a number of signal transduction pathways, including Sonic hedgehog (Shh) and platelet-derived growth factor (PDGF) signalling, the asynchrony in cilium formation could differentially influence the ability of the two daughter cells to respond to environmental signals and thereby their behaviour and fate specification. Furthermore, the strong microtubule anchorage activity associated with the centrosome retaining the older mother centriole would facilitate its anchorage to a specific site (for example, the VZ surface), thereby tethering the cell that inherits it. Indeed, we found that disruption of centriole maturation by removing Nin not only impairs asymmetric segregation of centrosomes, but also depletes radial glia progenitors from the VZ, a proliferative niche in the developing mammalian neocortex. Aside from their participation in microtubule organization and ciliogenesis, centrosomes associate with messenger RNAs (mRNAs)⁴⁶ and membrane-bound organelles such as the Golgi and recycling endosomes and regulate protein degradation^{47,48}, thereby raising the possibility that asymmetric centrosome inheritance might contribute to proper segregation of cell fate determinants to the two daughter cells of asymmetrically dividing progenitor/stem cells.

METHODS SUMMARY

In utero electroporation and photoconversion. *In utero* electroporation of the plasmids (for example, EGFP–CETN1) was performed as previously described^{49,50}. For *in utero* photoconversion, a similar surgical procedure was carried out as for *in utero* electroporation. The forebrain of the embryos that received electroporation was exposed to a brief (about three to five minutes) exposure of light at 350–400 nm while in the uterus. All procedures for animal handling and usage were approved by our institutional research animal resource centre (RARC).

Brain section, immunohistochemistry and imaging. Brains were fixed at the desired developmental stages and coronal sections were prepared using a vibratome (Leica Microsystems). Immunohistochemistry were performed as previously described⁵⁰. Images were acquired using a confocal laser scanning microscope (FV1000, Olympus) and analysed using FluoView (Olympus), Velocity (Improvision) and Photoshop (Adobe Systems). Data were presented as mean and s.e.m. and statistical differences were determined using nonparametric tests (Mann–Whitney–Wilcoxon test for two groups of data and Kruskal–Wallis test for three or more groups of data).

Cortical slice culture and time-lapse imaging. Cortical slice cultures were prepared and time-lapse imaging was acquired as previously described¹². Images were analysed using MetaMorph (Molecular Devices) and Photoshop (Adobe Systems).

Full Methods and any associated references are available in the online version of the paper at www.nature.com/nature.

Received 30 June; accepted 18 August 2009.

- Miyata, T., Kawaguchi, A., Okano, H. & Ogawa, M. Asymmetric inheritance of radial glial fibers by cortical neurons. *Neuron* **31**, 727–741 (2001).
- Noctor, S. C., Flint, A. C., Weissman, T. A., Dammerman, R. S. & Kriegstein, A. R. Neurons derived from radial glial cells establish radial units in neocortex. *Nature* **409**, 714–720 (2001).
- Malatesta, P., Hartfuss, E. & Gotz, M. Isolation of radial glial cells by fluorescent-activated cell sorting reveals a neuronal lineage. *Development* **127**, 5253–5263 (2000).
- Rakic, P. Elusive radial glial cells: historical and evolutionary perspective. *Glia* **43**, 19–32 (2003).
- Miyata, T. *et al.* Asymmetric production of surface-dividing and non-surface-dividing cortical progenitor cells. *Development* **131**, 3133–3145 (2004).
- Noctor, S. C., Martinez-Cerdeno, V., Ivic, L. & Kriegstein, A. R. Cortical neurons arise in symmetric and asymmetric division zones and migrate through specific phases. *Nature Neurosci.* **7**, 136–144 (2004).
- Chenn, A. & McConnell, S. K. Cleavage orientation and the asymmetric inheritance of Notch1 immunoreactivity in mammalian neurogenesis. *Cell* **82**, 631–641 (1995).
- Noctor, S. C., Martinez-Cerdeno, V. & Kriegstein, A. R. Distinct behaviors of neural stem and progenitor cells underlie cortical neurogenesis. *J. Comp. Neurol.* **508**, 28–44 (2008).
- Bornens, M. Centrosome composition and microtubule anchoring mechanisms. *Curr. Opin. Cell Biol.* **14**, 25–34 (2002).
- Doxsey, S., McCollum, D. & Theurkauf, W. Centrosomes in cellular regulation. *Annu. Rev. Cell Dev. Biol.* **21**, 411–434 (2005).
- Xie, Z. *et al.* Cep120 and TACCs control interkinetic nuclear migration and the neural progenitor pool. *Neuron* **56**, 79–93 (2007).
- Tsai, J. W., Bremner, K. H. & Vallee, R. B. Dual subcellular roles for LIS1 and dynein in radial neuronal migration in live brain tissue. *Nature Neurosci.* **10**, 970–979 (2007).
- Solecki, D. J., Model, L., Gaetz, J., Kapoor, T. M. & Hatten, M. E. Par6 α signaling controls glial-guided neuronal migration. *Nature Neurosci.* **7**, 1195–1203 (2004).
- Meraldi, P. & Nigg, E. A. The centrosome cycle. *FEBS Lett.* **521**, 9–13 (2002).
- Delattre, M. & Gonczy, P. The arithmetic of centrosome biogenesis. *J. Cell Sci.* **117**, 1619–1630 (2004).
- Lange, B. M. & Gull, K. A molecular marker for centriole maturation in the mammalian cell cycle. *J. Cell Biol.* **130**, 919–927 (1995).
- Nakagawa, Y., Yamane, Y., Okanou, T., Tsukita, S. & Tsukita, S. Outer dense fiber 2 is a widespread centrosome scaffold component preferentially associated with mother centrioles: its identification from isolated centrosomes. *Mol. Biol. Cell* **12**, 1687–1697 (2001).
- Bouckson-Castaing, V. *et al.* Molecular characterisation of ninein, a new coiled-coil protein of the centrosome. *J. Cell Sci.* **109**, 179–190 (1996).
- Ou, Y. Y., Mack, G. J., Zhang, M. & Rattner, J. B. CEP110 and ninein are located in a specific domain of the centrosome associated with centrosome maturation. *J. Cell Sci.* **115**, 1825–1835 (2002).
- Piel, M., Meyer, P., Khodjakov, A., Rieder, C. L. & Bornens, M. The respective contributions of the mother and daughter centrioles to centrosome activity and behavior in vertebrate cells. *J. Cell Biol.* **149**, 317–330 (2000).
- Anderson, C. T. & Stearns, T. Centriole age underlies asynchronous primary cilium growth in mammalian cells. *Curr. Biol.* doi:10.1016/j.cub.2009.07.034 (12 August 2009).
- Chretien, D., Buendia, B., Fuller, S. D. & Karsenti, E. Reconstruction of the centrosome cycle from cryoelectron micrographs. *J. Struct. Biol.* **120**, 117–133 (1997).
- Vorobjev, I. A. & Chentsov Yu. S. Centrioles in the cell cycle. I. Epithelial cells. *J. Cell Biol.* **93**, 938–949 (1982).
- Tsou, M. F. & Stearns, T. Mechanism limiting centrosome duplication to once per cell cycle. *Nature* **442**, 947–951 (2006).
- Cheng, J. *et al.* Centrosome misorientation reduces stem cell division during ageing. *Nature* **456**, 599–604 (2008).
- Yamashita, Y. M., Mahowald, A. P., Perlin, J. R. & Fuller, M. T. Asymmetric inheritance of mother versus daughter centrosome in stem cell division. *Science* **315**, 518–521 (2007).
- Rebollo, E. *et al.* Functionally unequal centrosomes drive spindle orientation in asymmetrically dividing *Drosophila* neural stem cells. *Dev. Cell* **12**, 467–474 (2007).
- Rusan, N. M. & Peifer, M. A role for a novel centrosome cycle in asymmetric cell division. *J. Cell Biol.* **177**, 13–20 (2007).
- Stevens, N. R., Raposo, A. A., Basto, R., St Johnston, D. & Raff, J. W. From stem cell to embryo without centrioles. *Curr. Biol.* **17**, 1498–1503 (2007).
- Cabernard, C. & Doe, C. Q. Stem cell self-renewal: centrosomes on the move. *Curr. Biol.* **17**, R465–R467 (2007).
- Spradling, A. C. & Zheng, Y. Developmental biology. The mother of all stem cells? *Science* **315**, 469–470 (2007).
- Yamashita, Y. M. & Fuller, M. T. Asymmetric centrosome behavior and the mechanisms of stem cell division. *J. Cell Biol.* **180**, 261–266 (2008).
- Gonzalez, C. Spindle orientation, asymmetric division and tumour suppression in *Drosophila* stem cells. *Nature Rev. Genet.* **8**, 462–472 (2007).

34. Cox, J., Jackson, A. P., Bond, J. & Woods, C. G. What primary microcephaly can tell us about brain growth. *Trends Mol. Med.* **12**, 358–366 (2006).
35. Higginbotham, H. R. & Gleeson, J. G. The centrosome in neuronal development. *Trends Neurosci.* **30**, 276–283 (2007).
36. Hinds, J. W. & Ruffett, T. L. Cell proliferation in the neural tube: an electron microscopic and golgi analysis in the mouse cerebral vesicle. *Z. Zellforsch. Mikrosk. Anat.* **115**, 226–264 (1971).
37. Chenn, A., Zhang, Y. A., Chang, B. T. & McConnell, S. K. Intrinsic polarity of mammalian neuroepithelial cells. *Mol. Cell. Neurosci.* **11**, 183–193 (1998).
38. Bornens, M. & Piel, M. Centrosome inheritance: birthright or the privilege of maturity? *Curr. Biol.* **12**, R71–R73 (2002).
39. Ando, R., Hama, H., Yamamoto-Hino, M., Mizuno, H. & Miyawaki, A. An optical marker based on the UV-induced green-to-red photoconversion of a fluorescent protein. *Proc. Natl Acad. Sci. USA* **99**, 12651–12656 (2002).
40. Salisbury, J. L., Suino, K. M., Busby, R. & Springett, M. Centrin-2 is required for centriole duplication in mammalian cells. *Curr. Biol.* **12**, 1287–1292 (2002).
41. Cai, L., Hayes, N. L. & Nowakowski, R. S. Local homogeneity of cell cycle length in developing mouse cortex. *J. Neurosci.* **17**, 2079–2087 (1997).
42. Mogensen, M. M., Malik, A., Piel, M., Bouckson-Castaing, V. & Bornens, M. Microtubule minus-end anchorage at centrosomal and non-centrosomal sites: the role of ninein. *J. Cell Sci.* **113**, 3013–3023 (2000).
43. Delgehr, N., Sillibourne, J. & Bornens, M. Microtubule nucleation and anchoring at the centrosome are independent processes linked by ninein function. *J. Cell Sci.* **118**, 1565–1575 (2005).
44. Bond, J. *et al.* A centrosomal mechanism involving CDK5RAP2 and CENPJ controls brain size. *Nature Genet.* **37**, 353–355 (2005).
45. Preble, A. M., Giddings, T. M. Jr & Dutcher, S. K. Basal bodies and centrioles: their function and structure. *Curr. Top. Dev. Biol.* **49**, 207–233 (2000).
46. Lambert, J. D. & Nagy, L. M. Asymmetric inheritance of centrosomally localized mRNAs during embryonic cleavages. *Nature* **420**, 682–686 (2002).
47. Wigley, W. C. *et al.* Dynamic association of proteasomal machinery with the centrosome. *J. Cell Biol.* **145**, 481–490 (1999).
48. Fuentealba, L. C., Eivers, E., Geissert, D., Taelman, V. & De Robertis, E. M. Asymmetric mitosis: unequal segregation of proteins destined for degradation. *Proc. Natl Acad. Sci. USA* **105**, 7732–7737 (2008).
49. Tabata, H. & Nakajima, K. Efficient *in utero* gene transfer system to the developing mouse brain using electroporation: visualization of neuronal migration in the developing cortex. *Neuroscience* **103**, 865–872 (2001).
50. Bultje, R. S. *et al.* Mammalian Par3 regulates progenitor cell asymmetric division via notch signaling in the developing neocortex. *Neuron* **63**, 189–202 (2009).

Supplementary Information is linked to the online version of the paper at www.nature.com/nature.

Acknowledgements We thank A. Hall, A. L. Joyner, K. V. Anderson, J. Kaltschmidt, B. M. Tsou, Y. Chin and L. A. McDowell for comments on the manuscript; members of the Shi laboratory for discussions; A. K. Hadjantonakis for human centrin 1 cDNA; M. Bornens for EGFP–Nin (mouse) and Nin truncation mutant plasmids; Y.-R. Hong for EGFP–Nin (human) plasmid; A. Miyawaki for pCS2+–Kaede plasmid; and H. Zhong, K. Svoboda and R. Tsien for DsRedexpress and mPlum cDNA constructs. We thank C. T. Anderson and T. Stearns for sharing unpublished data. This work is supported by grants from March of Dimes Birth Defects Foundation, Whitehall Foundation, Dana Foundation, Autism Speaks Foundation, Klingenstein Foundation, NARSAD (to S.-H.S.) and NIH (to S.-H.S. and R.B.V.).

Author Contributions X.W. and S.-H.S. conceived the project. X.W. performed most of the experiments. J.-W.T., W.-N.L. and R.B.V. contributed to the time-lapse imaging experiment and J.H.I. contributed to the characterization of Kaede–CETN1 co-localization and *in utero* photoconversion procedure. X.W. and S.-H.S. analysed data, interpreted results and wrote the manuscript. All authors edited the manuscript.

Author Information Reprints and permissions information is available at www.nature.com/reprints. Correspondence and requests for materials should be addressed to S.-H.S. (shis@mskcc.org).

METHODS

Plasmids and *in utero* electroporation and photoconversion. Human centrin 1 cDNA was obtained by polymerase chain reaction (PCR) and cloned into the KpnI and BamHI sites of pEGFP-C1 (Clontech) to generate the EGFP-CENTN1 plasmid. Kaede and DsRedexpress (DsRedex) cDNAs were obtained by PCR and cloned into pEGFP-CENTN1-C1 to replace EGFP in generating the Kaede-CENTN1 and DsRedex-CENTN1 plasmids. The mouse ninein (GenBank/EMBL/DBJ accession number AY515727) plasmid was provided by M. Bornens. Human ninein cDNA (IMAGE ID 3090109, Open Biosystems) was cloned into the EcoRI and NotI sites of pCDNA3.1. Three shRNA sequences against mouse *Nin* were designed as follows: shRNA-a (5'-GCAGAAGGCCAGCTGAGGT-3'), shRNA-b (5'-GGCCGAGATCCGGCACTTG-3'), shRNA-c (5'-GCTTCAATT CAGACAATGG-3'). All sense and antisense oligonucleotides were purchased from Sigma. Annealed oligonucleotides were cloned into the HpaI and XhoI sites of the lentiviral vector pLL3.7, which contains a separate CMV promoter that drives expression of EGFP⁵⁰. In this study, mouse *Nin* shRNA-c was primarily used after extensive characterization to demonstrate that it specifically suppressed *Nin* protein expression and function. For siRNA experiments, synthetic oligonucleotides against *Nin* and control were purchased from Santa Cruz Biotechnology (sc-61196). Human *NIN* cDNA, which differs from mouse *Nin* cDNA in the shRNA-c targeting region and is thereby insensitive to *Nin* shRNA-c expression, was used for the rescue experiment. The N terminus (nucleotides 1–1120) and C-terminus (nucleotides 5623–6339) of mouse *Nin* were amplified by PCR and cloned into the EcoRI and NotI sites of pCAG-IRES-EGFP. All plasmids were confirmed by sequencing.

In utero electroporation was performed as previously described^{49,50}. In brief, a timed pregnant CD-1 mouse at 13.5 days of gestation (E13.5) or a rat at E16.5 was anaesthetized, the uterine horns were exposed, and ~1 µl of plasmid DNA (1–3 µg µl⁻¹) mixed with Fast Green (Sigma) was manually microinjected through the uterus into the lateral ventricle, using a bevelled and calibrated glass micropipette (Drummond Scientific). For electroporation, five 50-ms pulses of 40–50 mV with a 950-ms interval were delivered across the uterus with two 9-mm electrode paddles positioned on either side of the head (BTX, ECM830). For *in utero* photoconversion, a similar surgical procedure was carried out as for *in utero* electroporation. The forebrain of the embryos that received electroporation was exposed to a brief (about 3 to 5 min) exposure of light at 350–400 nm while in the uterus. Throughout these surgical procedures, the uterus was constantly bathed with warm PBS (pH 7.4). After the procedure, the uterus was placed back in the abdominal cavity and the wound was surgically sutured. The animal was then placed in a 28 °C recovery incubator under close monitoring until it recovered and resumed normal activity. All procedures for animal handling and usage were approved by our institutional research animal resource centre (RARC).

Brain sectioning and confocal imaging and analysis. Embryos were removed and transcardially perfused with ice-cold PBS (pH 7.4) followed by 4% paraformaldehyde in PBS (pH 7.4). For cell cycle exit analysis, electroporated embryos were exposed to bromodeoxyuridine (BrdU, ~50–100 mg kg⁻¹ body weight) for

24 h before being killed. Brains were dissected out and coronal sections were prepared using a vibratome (Leica Microsystems). For immunohistochemistry, sections were incubated for 1 h at room temperature in a blocking solution (10% normal goat or donkey serum as appropriate, 0.1% Triton X-100, and 0.2% gelatin in PBS), followed by incubation with the primary antibodies overnight at 4 °C. Sections were then washed in 0.1% Triton X-100 in PBS and incubated with the appropriate secondary antibody for 1–2 h at room temperature.

The primary antibodies used were: rabbit polyclonal anti-γ-tubulin (Sigma, 1:500), mouse monoclonal anti-pericentrin 1 (BD Biosciences, 1:1,000), mouse monoclonal anti-β-III tubulin (clone TUJ1) (Covance, 1:500), rabbit polyclonal anti-Pax6 (Covance, 1:500), rabbit polyclonal anti-Tbr2 (Millipore/Chemicon, 1:500), rat monoclonal anti-BrdU (Abcam, 1:400), mouse polyclonal anti-Ki67 (Novus Biological, 1:200), rabbit polyclonal anti-GLAST (Invitrogen, 1:400), rabbit polyclonal anti-phospho-histone 3 (Millipore/Upstate, 1:1,000), mouse monoclonal anti-phospho-H2AX (Millipore/Upstate, 1:250) and rabbit polyclonal anti-cleaved caspase 3 (Cell Signaling Technology, 1:250). Secondary antibodies used were: goat or donkey anti-mouse or anti-rabbit Alexa-546 and Alexa-647 conjugated antibodies (Invitrogen/Molecular Probes, 1:500). DNA was stained with 4',6-diamidino-2-phenylindole (DAPI) (Invitrogen/Molecular Probes). Images were acquired with an Olympus FV1000 confocal microscope, and analysed with FluoView (Olympus), Volocity (Improvision) and Photoshop (Adobe Systems).

Data are presented as mean ± s.e.m. and nonparametric tests (Mann-Whitney–Wilcoxon test for two groups of data and Kruskal–Wallis test for three or more groups of data) were used for statistical significance estimation.

Cortical slice culture and time-lapse imaging. Cortical slice cultures were prepared and time-lapse imaging was acquired as previously described¹². About 12 h after *in utero* electroporation, embryos were removed and the brain was extracted into ice-cold artificial cerebro-spinal fluid (ACSF) containing (in mM): 125 NaCl, 5 KCl, 1.25 NaH₂PO₄, 1 MgSO₄, 2 CaCl₂, 25 NaHCO₃ and 20 glucose; pH 7.4, 310 mOsm l⁻¹. Brains were embedded in 4% low-melting agarose in ACSF and sectioned at 400 µm using a vibratome (Leica microsystems). Brain slices that contained Kaede-CENTN1- and mPlum-expressing cells were transferred on to a slice culture insert (Millicell) in a glass-bottom Petri dish (MatTek Corporation) with culture medium containing (by volume): 66% BME, 25% Hanks, 5% FBS, 1% N-2, 1% penicillin/streptomycin/glutamine (Invitrogen/GIBCO) and 0.66% D-(+)-glucose (Sigma). Cultures were maintained in a humidified incubator at 37 °C with constant 5% CO₂ supply. Twenty-four hours later, Petri dishes with slice cultures were transferred to an inverted microscope DMIRB (Leica) with a ×10 objective and the slices were exposed to brief (~12 s) epifluorescent illumination using a DAPI filter. The slices were returned to the incubator and cultured for another 24 h. Time-lapse images of dividing radial glia cells expressing Kaede-CENTN1 and mPlum were acquired using a ×40 objective lens and a CoolSnap HQ camera (Roper Scientific) every 10 min for about 5 to 8 h. Images were analysed using MetaMorph (Molecular Devices) and Photoshop (Adobe Systems).